

Nanostructure Zinc Oxide with Cobalt Dopant by PLD for Gas Sensor Applications

A.A. Yousif¹, N.F. Habubi^{1,*}, A.A. Haidar²

¹ Department of Physics, College of Education, University of Al-Mustansiriyah, Baghdad, Iraq

² School of Applied Sciences, University of Technology, Baghdad, Iraq

(Received 17 February 2012; published online 07 May 2012)

The present paper is based on study of polycrystalline ZnO:Co thin films deposited on glass substrates by pulsed laser deposition (PLD) technique using pulsed Nd-YAG laser with wavelength ($\lambda = 532$ nm) and duration (7 ns) and energy fluence (1.4 J/cm²) with different doping (1 wt. %, 3 wt. % and 5 wt. %). The X-Ray diffraction patterns of the films showed that the ZnO films and ZnO:Co films exhibit wurtzite crystal structure and high crystalline quality. The root mean square (RMS) surface roughness of Co doped ZnO thin films was estimated using atomic force microscopy (AFM) found to be 50.95 nm, 55.78 nm, 56.94 nm and 67.88 nm for pure, 1 wt. %, 3 wt. % and 5 wt. % Co doping concentrations respectively. Through the electrical properties, electrical D.C conductivity at temperature range (27-300) °C for ZnO:Co films as studied which are realized that these films have two activation energies. Hall effect is studied to estimate the type of carriers, from the result we deduced that the ZnO:Co thin films are *n*-type. The films exhibited good sensitivity to the ethanol vapors with quick response-recovery characteristics and it was found that the sensitivity for detecting (80) ppm, for ethanol vapor was of (27.5), (31.75), (79.0) and (53.1) at an operating temperature of (50) °C for ZnO:Co thin films.

Keywords: Pulsed-Laser, Zinc Oxide Thin Films, Structural, Electrical, Morphology, Gas Sensor.

PACS numbers: 78.66.Bz, 81.40.Vw.

1. INTRODUCTION

Zinc oxide (ZnO) is an *n*-type semiconductor of wurtzite structure, with a direct band gap of about 3.37 eV at room temperature [1, 2]. It is a quite important oxide which exhibits near ultraviolet emission and transparent conductivity. ZnO is piezoelectric due to its non-central symmetry, a property that makes it a major candidate for building electromechanical coupled sensors and transducers [3]. ZnO is also one of the most widely applied oxide gas sensing materials [4]. Various deposition techniques have been developed for depositing ZnO thin films, including chemical vapor deposition, radio frequency sputtering, magnetron sputtering, sol-gel, ion-beam-assisted or molecular-beam epitaxy, and pulsed laser deposition (PLD).[5] Amongst them, the pulsed laser deposition technique is interesting because it offers an easy way to add other elements for alloying or for doping purposes. An important point is that PLD gives the advantage of carrying out the growth in a high-O partial pressure for better control of possible oxygen deficiency [6]. The possibility to tune the deposition parameters in order to control the morphology of the deposited films, for example passing from smooth to rough films or to nanostructures, is a fundamental issue towards their functional use in the different technological fields. Here we report on the growth of zinc oxide films with different morphologies by pulsed laser deposition, using different substrate temperatures. The possible growth mechanisms are discussed in order to explain the different observed morphologies. [7-9] In this study we prepared Co-doped ZnO thin films deposited by PLD on glass substrates at 400 °C temperature. We also investigate the influence of laser (1.4 J/cm²) applied during the deposition process on the structural, optical, electrical and sensing properties of the films.

2. EXPERIMENT DETAILS

ZnO:Co thin films were synthesized by pulsed laser deposition system using a second harmonic Nd:YAG laser. Thin films were grown in a vacuum chamber with background pressure of $\sim 1 \times 10^{-3}$ mbar. The Nd:YAG laser was operated at the wavelength of ($\lambda = 533$ nm) with the repetition rate of (10 Hz) and pulse duration of (7 ns). The target to substrate distance was (3 cm). X-ray diffraction measurement has been done and compared with the ASTM (American Society of Testing Materials) cards, using Philips PW 1840 X-ray diffract meter of $\lambda = 1.54$ Å from Cu-K α . The morphological features of the various films were investigated with a JEOL JSM-6360 equipped with a EDAX detector. The microstructures of the films were analyzed using Atomic Force Microscopy (AFM-Digital Instruments Nan Scope) working in tapping mode. The resistivity is conventionally calculated from measured electrical resistance. The activation energy is calculated from measuring the conductivity as a function of temperature using a cryostat. The temperature read out is by (MANFREDI L7C). The bias voltage was supplied by (FARNELL E 350) power supply. The current read out is by (Kithley-616 Digital Electrometer) multimeter. Hall coefficient (RH), determine the type of charge carriers and estimate their concentration and mobility measurement. The measurement begins after the vertical application of magnetic field density of 0.25 Tesla (Wb/m²) on the film. At this point, the measurement is made by changing the current flowing in the film which, in turn, is achieved by changing the applied potential difference through the power supply. Power supply type Tandem. They are connected in series with an Ammeter type Kithley-616 Digital Electrometer; the other two electrodes are connected with the same type of copper wires, to voltmeter type Kithley. 177 Micro Voh Dmm. The sensing measurements were carried out by

* nadirfadhil@yahoo.com

measuring the variation in resistivity through measuring the output current resulting from exposing the thin film surface to the gas or chemical vapor (methanol and ethanol) Ethanol (laboratory reagents 99.9 %) and methanol (laboratory reagents 99.95 %) were evaporated by heating them to 50 °C, the temperature was recorded by a k-type thermocouple (XB 9208B). The bias voltage was supplied by (FARNELL E350) power supply. The output current was recorded by (Kithley-619 Electrometer) multimeter. The thin film surface exposed to 80 ppm vapor concentrations in vacuum of ethanol and methanol. The measuring carried out with an applied voltage constant to (5) volts at temperature constant of 50 °C.

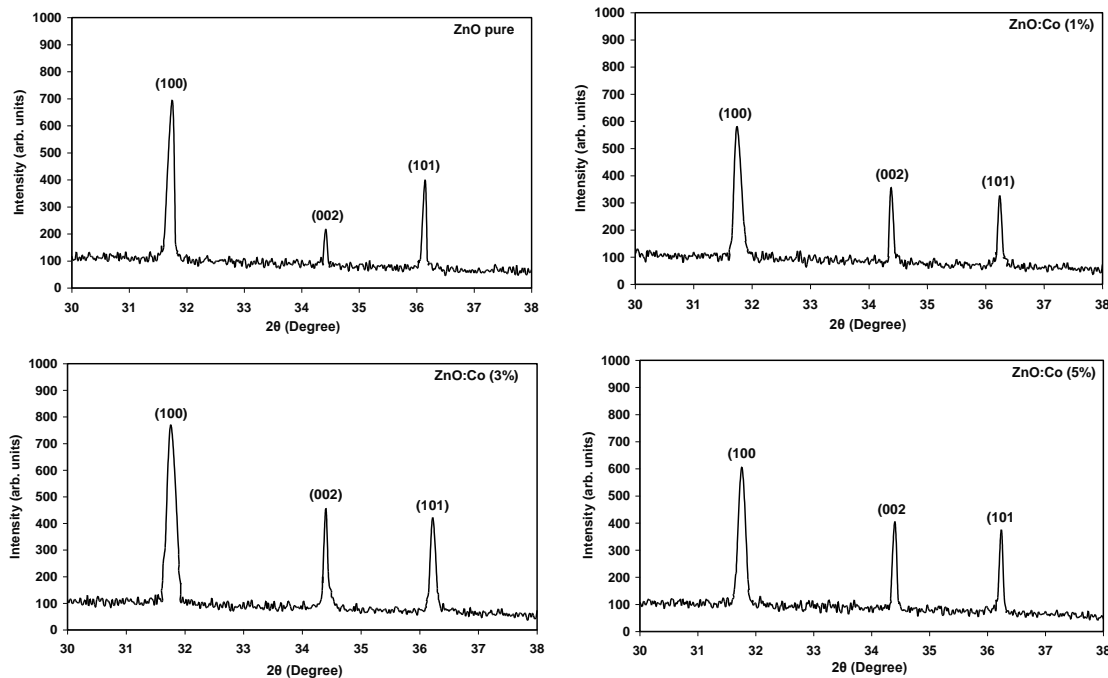


Fig. 1 – XRD spectrum of ZnO pure and cobalt-doped ZnO thin films deposited on glass substrate

3.2 Morphology Properties

Fig. 2 show the AFM images of samples which indicate the formation of grains, hence revealing the crystalline nature of the thin films. The surface morphology of the undoped and ZnO:Co films as observed from the AFM micrographs. Fig. 2, left pictures proves that the grains are uniformly distributed within the scanning area (10×10) μm , with individual columnar grains extending upwards. The root mean square (RMS) surface roughness of Co doped ZnO films are found to be 50.95 nm, 55.78 nm, 56.94 nm and 67.88 nm for pure, 1wt. %, 3wt. % and 5wt. % Co doping concentrations respectively (can be see Table 1), i.e. the root mean square (RMS) surface roughness exponentially increases with the dopant concentration. The 3D-AFM right pictures of pure and dopant are shown in Fig. 2. It is seen that no segregation of dopants is observed in the grain boundaries of the doped films.

From AFM images we found that the presence of the ZnO:Co films increases the (RMS) roughness in the films Figures. The higher the root mean square (RMS) roughness was found for ZnO:Co films which have compressive

3. RESULTS AND DISCUSSION

3.1 Structural Properties

Fig. 1 shows the XRD patterns of ZnO:Co films. It can be seen that the structure of all the films are hexagonal with a strong (100) preferred orientation.

No diffraction peaks of Co or other impurity phases are found in these samples. The angle of the dominant peak corresponding to (100) plane is at $2\theta = 31.7^\circ$ for the undoped ZnO sample and it increased as the concentration of Co impurity increased [10].

stress and lower root mean square (RMS) roughness for ZnO film which have tensile stress [11-13].

Table 1 – AFM characteristics of the ZnO (undoped and Co doped) films deposited at 400 °C substrate temperature, 1.4 J/cm² laser energy and 10^{-1} mbar Oxygen pressure

Co dopant content in the target, wt. %	RMS [nm] taken from $10 \times 10 \mu\text{m}$
ZnO-pure	50.95
ZnO:Co (1 %)	55.78
ZnO:Co (3 %)	56.94
ZnO:Co (5 %)	67.88

3.3 Electrical Properties

3.3.1 D.C. Electrical Conductivity

The conductivity of ZnO:Co films decreased as the value of $1/T$ increases at higher temperature ($T > 27^\circ\text{C}$), suggesting a thermally activated conduction in this temperature range. The conductivity for undoped about $1.587 (\Omega\cdot\text{cm})^{-1}$ of Co increases in doping have concentrations (1wt. % and 3wt. %) decreases the conductivity

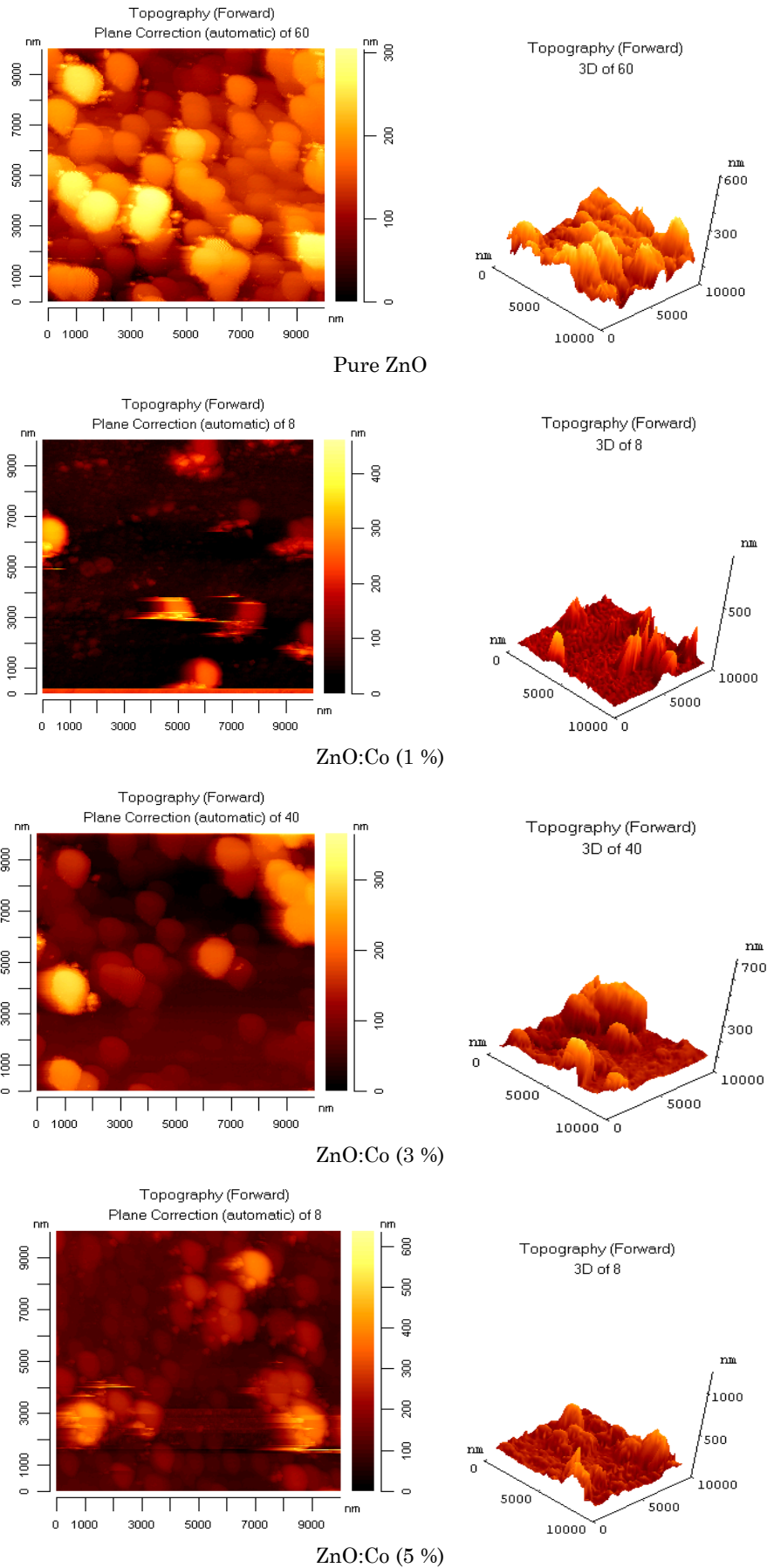


Fig. 2 – The AFM images of samples

to $1.052 (\Omega \cdot \text{cm})^{-1}$ of concentrations (5wt. %) for samples is presented in Table 2 [14, 15].

Table 2 – Electrical properties of ZnO thin films prepared at different Co dopant concentrations

Sample	β ($\Omega \cdot \text{cm}$)	σ , ($\Omega \cdot \text{cm}$) ⁻¹ at RT	$ R_H $	N , (cm^{-3})	μ , (cm ² / v.s)
ZnO-pure	0.630	1.587	48.8	1.28×10^{17}	77.13
ZnO:Co (1%)	0.351	2.845	17	3.6×10^{17}	48.36
ZnO:Co (3%)	0.366	2.731	0.13	4.56×10^{19}	0.374
ZnO:Co (5%)	0.949	1.052	36	1.7×10^{17}	37.87

3.2.2 Activation Energy

Fig. 3 shows the electrical activation energy of ZnO:Co films are calculated from $\ln\sigma$ versus $(1000/T)$ plots for different Co-doping concentrations. As shown

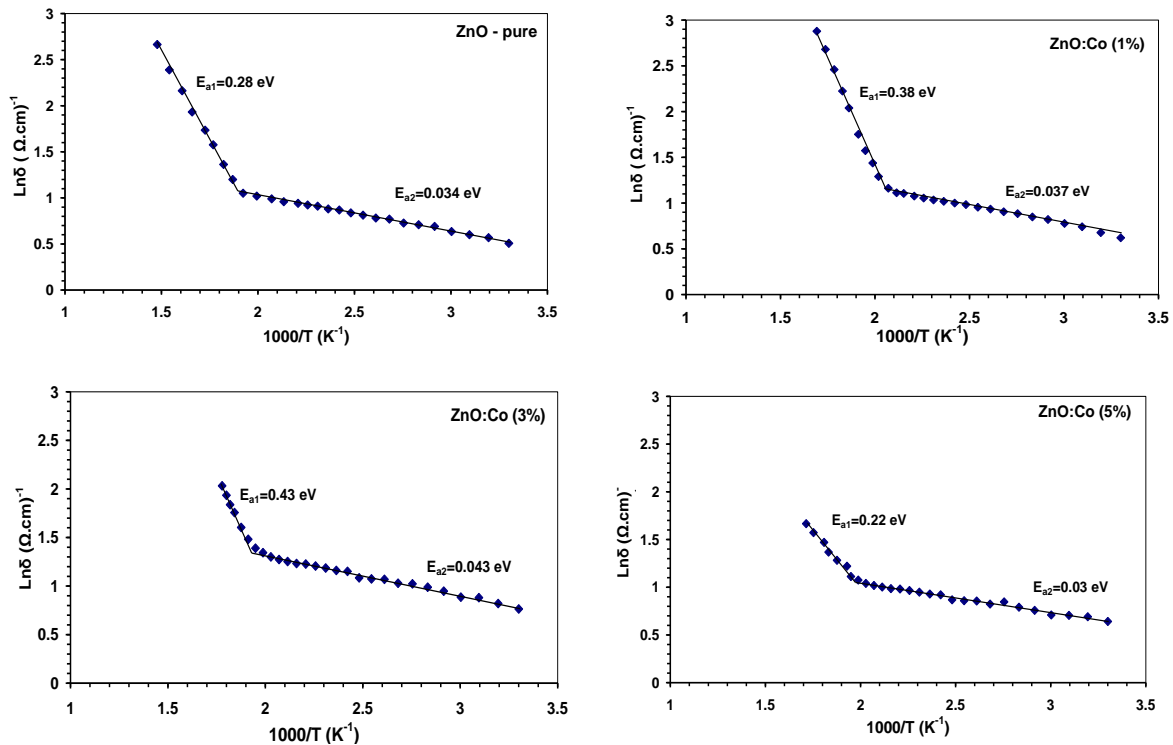


Fig. 3 – $\ln\sigma$ versus $1000/T$ for pure ZnO and ZnO:Co films at different doping concentrations and temperatures

3.3.3 Hall Effect

The results obtained from Hall effect show that the pure ZnO and ZnO:Co films were *n*-type, this goes in agreement with the previous work [17-19]. Hall voltage values decrease when the current increases, as shown in Fig. 4. It is noticed that the field applied to the film ends has a proportional relationship with Hall voltage.

The values of R_H at different concentrations of Co are given in Table 2, the variations of N and μ_H with Co concentration in ZnO:Co films are shown in Table 2. It is seen from this table that N increase with increasing Co concentration. Maximum values of N ($4.56 \times 10^{19} \text{ cm}^{-3}$) are obtained for 3wt. % of Co, but the N decreases

in Table 3. The activation energy depends on the doping and it will be increased with increasing doping until 3wt. %, then, began to decrease. The value of activation energy for the as deposited ZnO film and for the

Table 3 – Activation energy of ZnO thin films prepared at different Co dopant concentrations

Sample	Ea_1 (eV)	Ea_2 (eV)
ZnO-pure	0.28	0.034
ZnO:Co (1 %)	0.38	0.037
ZnO:Co (3 %)	0.43	0.043
ZnO:Co (5 %)	0.22	0.03

Co-doped ZnO films its values. The activation energy depends on the donor carrier concentration and the impurity energy levels. An increase in donor carrier concentration brings the Fermi level up in the energy gap and results in the decrease of activation energy [16].

es when increasing Co doping to Co 5wt. %.

The mobility μ_H of the ZnO:Co films decreases with increasing dopant concentration as in Table 2, and reaches a minimum around Co 3wt. % with a value of $0.374 \text{ cm}^2 \text{ V}^{-1} \text{ S}^{-1}$.

3.4 Gas Sensor

Fig. 5 and Fig. 6, show the sensitivity as functions of operation time at a temperature of 50°C . Zinc oxide pure and ZnO:Co films were placed under 80 ppm ethanol and methanol vapor concentration. Fig. 5 show, an increase in sensitivity value as the doping percentage increase except 1wt. % Co doping which was less

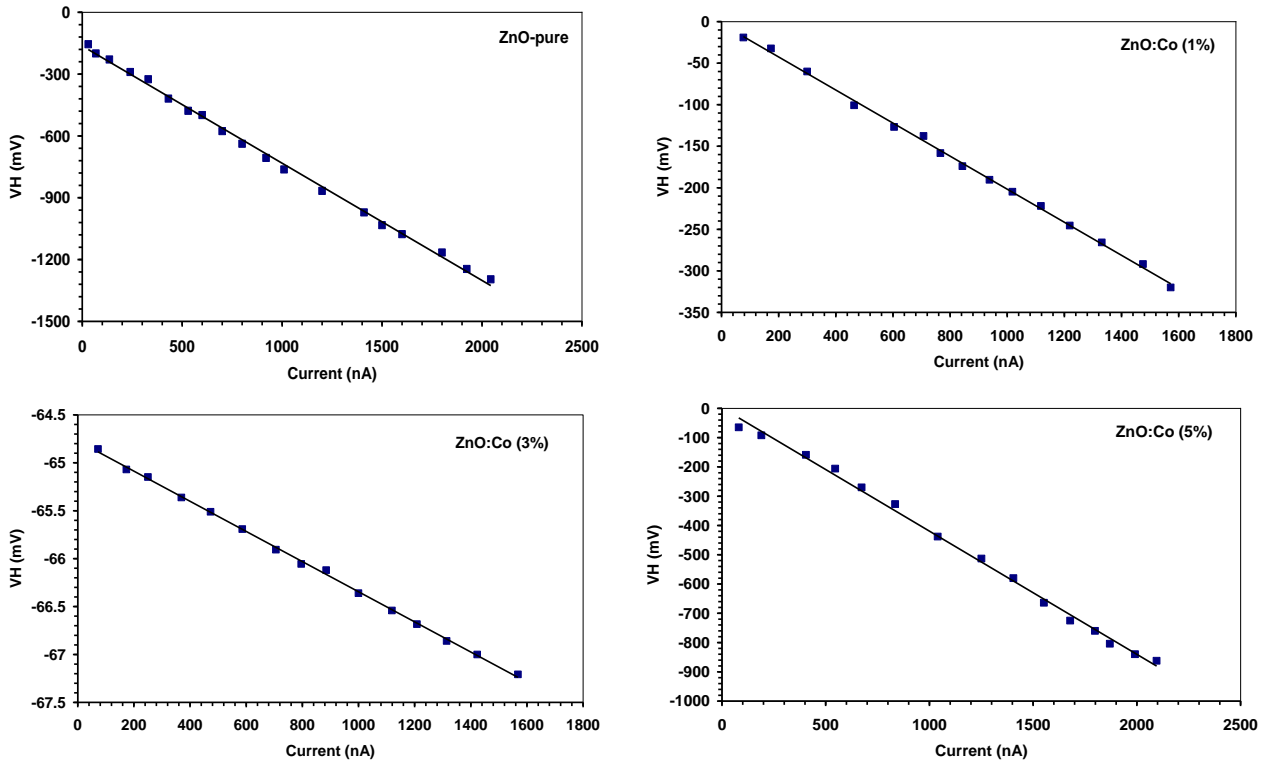


Fig. 4 – Relation between Hall voltage (V_H) and the current (I) of ZnO thin films prepared at different Co dopant concentrations

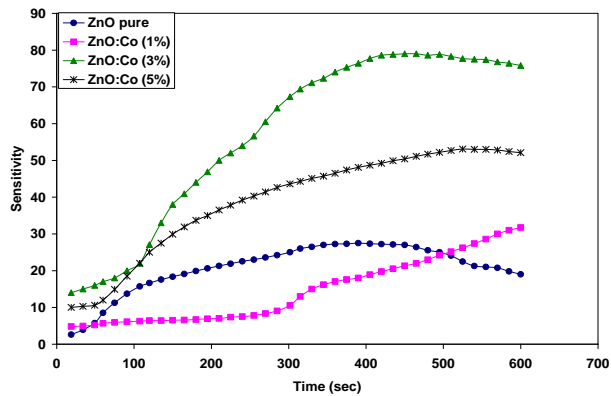


Fig. 5 – Sensitivity for as-deposited ZnO:Co as function of operation time for Ethanol

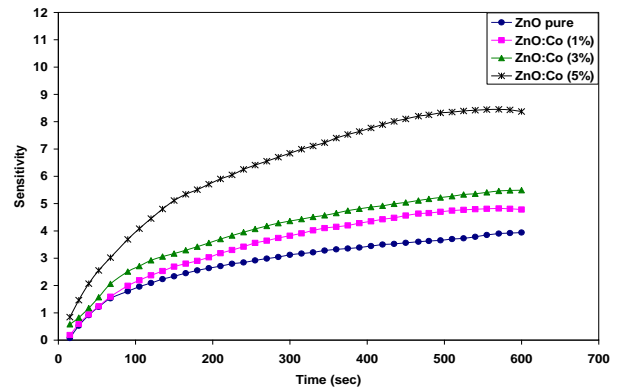


Fig. 6 – Sensitivity for as-deposited ZnO:Co as a function operation time for methanol

than the pure while the response 5wt. % and 3 % were above the pure value. Furthermore, ethanol gas sensor showed high sensor signal and fast response at concentration 80 ppm with operating temperature of 50 °C in ZnO:Co thin films. The increase in sensitivity values are higher than that of undoped ZnO film [20, 21].

Fig. 6, show the sensitivity as a functions of operation time at a temperature of 50 °C for the various impurity for ZnO:Co films under 80 ppm methanol vapor concentration, were increase in the sensitivity as the dopant concentration of Co increases.

4. CONCLUSION

The structures, morphology, electrical and sensing properties of ZnO: Co films for an ethanol and methanol vapor gas sensor obtained by PLD system were investigated: we conclude the following:

1. The crystal structure of the films is hexagonal wurtzite. All films are polycrystalline and (100) oriented.

2. It was found that doped ZnO films with good structural and morphological properties can be deposited at $x = 0.05$. The film deposited at an optimum alumina concentration 0.05 exhibited more intensity maintaining average RMS roughness of (50.95-67.88) nm respectively. The increase of the dopant concentration into the target increases the toughness of the as deposited films.

3. By studying the electrical properties, electrical D.C conductivity at temperature range (27-300) °C for pure and different doping (1 wt. %, 3 wt. % and 5 wt. %), we realized that these films have two activation energies. Hall effect is studied to estimate the type of carriers, from the result we deduced that the pure ZnO and the doped ZnO:Co films are n -type.

4. The pure ZnO and ZnO: Co thin films sensors

show good measurable response to methanol in a concentration of (80) ppm, with a maximum response at operation temperature of (50) °C were (4.0), (4.84), (5.5) and (8.45), respectively. The sensors with higher resistance yields higher response to the gas under test.

REFERENCES

1. M. Sucheai, S. Christoulakis, M. Katharakis, G. Kiriakidis, N. Katsarakis, E. Koudoumas, *Appl. Surf. Sci.* **253**, 8141 (2007).
2. Y. Chen, D. Bagnall, T. Yao, *Mater. Sci. Eng. B* **75**, 190 (2000).
3. U. Ozgur, I. Ya, C. Alivov, A. Liu, M.A. Teke, S. Reshchikov, V. Dogan, S. Avrutin, H. Cho, H. Morkoc, *J. Appl. Phys.* **98**, 041301 (2005).
4. T. Seiyama, A. Kato, K. Fujiishi, M. Nagatani, *Anal. Chem.* **34**, 1502 (1962).
5. R. Ayouchi, L. Bentes, C. Casteleiro, O. Conde, C.P. Marques, E. Alves, A.M.C. Moutinho, H.P. Marques, O. Teodoro, R. Schwarz, *Appl. Surf. Sci.* **255**, 5917 (2009).
6. A. Fouchet, W. Prellier, B. Mercey, L. Mechin, V.N. Kulkarni, T. Venkatesan, *J. Appl. Phys.* **96**, 3228 (2004).
7. D. Valerini, A.P. Caricato, A. Creti, M. Lomascolo, F. Romano, A. Taurino, T. Tunno, M. Martino, *Appl. Surf. Sci.* **255**, 9680 (2009).
8. D. Valerini, A.P. Caricato, M. Lomascolo, F. Romano, A. Taurino, T. Tunno, M. Martino, *Appl. Phys. A-Mater.* **93**, 729 (2008).
9. R.P. Doherty, Y.K. Sun, Y. Sun, J.L. Warren, N.A. Fox, D. Cherns, M.N.R. Ashfold, *Appl. Phys. A-Mater.* **89**, 49 (2007).
10. D.R. Uhlmann, H.K. Bowen, W.D. Kingery, *Introduction to Ceramics* (New York: John Wiley & Sons Inc: 1976).
11. D.C. Look, J. W. Hemsley, J.R. Rozdove, *Phys. Rev. Lett.* **82**, 2552 (1999).
12. K.-S. Weibenrieder, J. Muller, *Thin Solid Films* **300**, 30 (1997).
13. G. Sberveglieri (Ed.), *Gas sensors, Principles, Operation and Developments* (Kluwer Academic Publications: 1992).
14. R. Maity, S. Kundoo, K.K. Chattopadhyay, *Sol. Energ. Mat. Sol. C.* **86**, 217 (2005).
15. D.R. Patil, L.A. Patil, *Sensors & Transducers Journal*, **81** No7, 1354 (2007).
16. R. Kumar, N. Khare, *Thin Solid Films* **516**, 1302 (2008).
17. A.V. Singh, Manoj Kumar, R.M. Mehra, Akihiro Wakahara, Akira Yoshida, *J. Indian Inst. Sci.* **81**, 527 (2001).
18. M. Novotny, J.R. Duclere, E. McGlynn, M.O. Henry, R. O'Haire, J.-P. Mosnier, *J. Phys. Conf. Ser.* **59**, 505 (2007).
19. M. Girtan, G.G. Rusu, S. Dabos-Seignon, M. Rusu, *Appl. Surf. Sci.* **254**, 4179 (2008).
20. D. Dimova-Malinovska, H. Nichev, V. Georgieva, O. Angelov, J.-C. Pivin, V. Mikli, *Phys. Status Solidi A* **205**, 1993 (2008).
21. H. Nichev, O. Angelov, J. Pivin, R. Nisumaa, D. Dimova-Malinovska, *J. Phys. Conf. Ser.* **113**, 012035 (2008).